Exacta
ISSN: 1678-5428
exacta@uninove.br
Universidade Nove de Julho
Brasil

Alves Bandeira, Alex; Pimenta, Paulo M.; Wriggers, Peter
A 3D contact investigation of rough surfaces considering elastoplasticity
Exacta, vol. 6, núm. 1, enero-junio, 2008, pp. 109-118
Universidade Nove de Julho
São Paulo, Brasil

A 3D contact investigation of rough surfaces considering elastoplasticity

Alex Alves Bandeira
Professor Doctor of the Department of Civil Engineering – Mackenzie; Professor Doctor of the Department of Civil Engineering – Uninove.
São Paulo – SP [Brazil]
alex_bandeira@terra.com.br

Paulo M. Pimenta
Titular Professor of the Department of Structural Engineering; Polytechnic School at Universidade de São Paulo.
São Paulo – SP [Brazil]
ppimenta@usp.br

Peter Wriggers
Titular Professor of the Institute for Structural and Computational Mechanics – University of Hannover.
Hannover [Germany]
wriggers@ibnm.uni-hannover.de

In this work, the non-penetration condition and the interface models for contact, taking into account the surface microstructure, are investigated in detail. It is done using a homogenization procedures presented by Bandeira, Wriggers and Pimenta (2001a), to obtain by numerical simulation the interface behavior for the normal and tangential contact pressures, based on statistical surface models. The contact surfaces of both bodies are rough. This paper can be regarded as a complementary study to that presented by Bandeira, Wriggers and Pimenta (2006). Here, the plasticity of the asperities is taken into account by assuming a constitutive equation based on an associated von Mises yield function formulated in principal axes. The plastic zones in the microstructure are shown to study in detail the contact interface. Numerical examples are selected to show the ability of the algorithm to represent interface law for rough surfaces, considering elastoplastic behaviour of the asperities.

Key words: Contact mechanics. Contact surface. Elastoplasticity. Interface constitutive equation.

1 Introduction

Several formulations concerning the treatment of the contact interface have been presented in the literature, especially when the contact interface of two contacting bodies is rough. Constitutive equations for the normal contact have been developed by investigating micromechanical behavior within the contact surface. Associated models have been developed based on experiments (GREENWOOD; WILLIAMSON, 1966; EVSEEV; MEDVEDEV; GRIGORIYAN, 1991; ZAVARISE; SCHREFLER; Wriggers, 1992; YOVANOVICH, 1981; KRAGELSKY; DOBYCHIN; KOMBALOV, 1982). In general, the micromechanical behavior depends on material parameters, like hardness, and on geometrical parameters, like surface roughness. It should be noted that the real micromechanical phenomena are extremely complex due to extremely high local pressure at the asperities. The model used in this paper attempts only to capture the most important phenomena and assume either elastic or plastic deformation of the asperities having real contact in the interface.

This article concentrates on the behavior of the contact interface. The idea is to study the interface behavior by modeling the contact surfaces, using a finite element discretization, to take into account the geometrical properties of the microstructure. The probabilistic theory is applied based on a statistical model of the micro geometry, like in the microscopic contact mechanics developed by Greenwood and Williamson (1966), and by Wriggers and Vu Van and Stein (1990). Finally, a simple homogenization leads to a contact interface law.

A three-dimensional eight-node brick element is used for the treatment of finite elastic-plastic deformation of the contacting surfaces, (KARDESTUNCER; NORRIE, 1987). An augmented Lagrangian method is applied to solve the frictional contact problems, because high-pressures occur which cannot be treated adequately by standard penalty procedures (BERTSEKAS, 1984, 1995; FLETCHER, 2000; LUENBERGER, 1984; LAURSEN; MAKER, 1995; LAURSEN; SIMO, 1993a, 1993b; WRIGGERS; SIMO, 1985; WRIGGERS; SIMO; TAYLOR, 1985; WRIGGERS; VU VAN; STEIN, 1990; WRIGGERS; ZAVARISE, 1993; HEEGAARD; CURNIER, 1993). The technique used to solve three-dimensional contact problems with friction, in finite deformations (CURNIER, 1984; TABOR, 1981) was already developed and described in Bandeira, Wriggers and Pimenta (2001a, 2001b, 2003, 2006); Simo and Laursen (1992); Wriggers (1995), Wriggers and Simo (1985); Wriggers, Simo and Taylor (1985); Wriggers, Vu Van and Stein (1990); Wriggers and Zavarise (1993); Alart and Curnier (1991); Oden and Pires (1983).

The finite element program is based on a C++ code, developed by Bandeira, Wriggers and Pimenta (2006). All numerical examples given are based on three-dimensional calculations. In the numerical examples, high-density meshes are used to represent the geometrical irregularity on the surfaces more precisely.

2 Constitutive equation for contact interface

Different approaches have been proposed to represent microscopic contact mechanisms. The available formulations are based either on curve fitting of experimental results or on theoretical analyses of microscopically rough surface (GREENWOOD; WILLIAMSON, 1966; EVSEEV; MEDVEDEV; GRIGORIYAN, 1991; ZAVARISE; SCHREFLER; WRIGGERS, 1992; KRAGELSKY; DOBYCHIN; KOMBALOV, 1982).

In this paper, the current normal approach g_N is investigated in detail. It can be defined by

$$g_N = \xi - d \tag{2.1}$$

where ξ denotes the maximum initial asperities height and d the current mean plane distance. Thefigureal interpretation of equation (2.1) is illustrated in Figure 1.

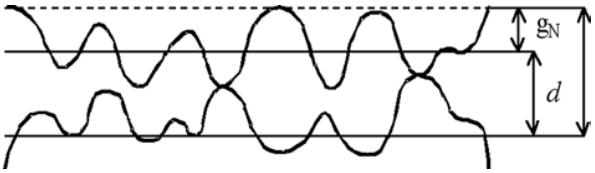

Figure 1: Physical approach on the contact interface (cross section)
Source: Bandeira, 2004.

The normal contact force F_N is obtained as a product of the apparent pressure by the apparent contact area A, as follows:

$$F_N = A \cdot c_N \cdot (g_N)^2 \tag{2.2}$$

where c_N is defined by the penalty parameters of the augmented Lagrangian algorithmic. Following relationship correlates the current normal approach g_N with the apparent mechanical pressure P_N:

$$P_N = c_N \cdot (g_N)^2 \tag{2.3}$$

The mechanical constants mentioned in (2.2) depend on the micromechanics of the surface. This constitutive equation was presented in Zavarise, Schrefler and Wriggers (1992).

3 A simple homogenization method for contact interface

The basic aim of this paper is to derive constitutive contact laws, as stated in Section 2, for a rough surface by using the finite element method. For this purpose, one has to model and discretize the rough surface and then, by homogenization procedures, to develop an interface law for contact. This section summarizes the homogenization method leading to the contact interface laws. The interface law is obtained from numerical simulation, using a model that consists of two deformable bodies in contact (Figure 2).

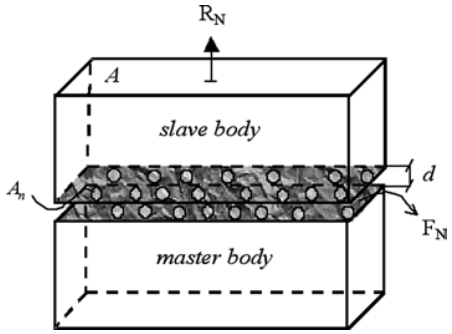

Figure 2: Model to obtain an interface law
Source: Bandeira, 2004.

The contact surfaces of both bodies are rough. A representative surface at the contact interface is represented by the Figure 3.

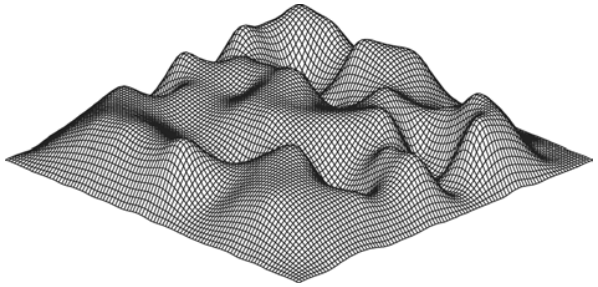

Figure 3: Contact surface with macroscopic asperities
Source: Bandeira, 2004.

The procedure to find the associated interface law is performed in several steps. The bodies are discretized using standard hexahedral finite elements. One body is placed above another with initial distance to separate them. The inferior body is kept fixed in position and superior body is moved

towards the inferior body by a displacement imposed on the top surface A. The fixed block is defined as master body and one that is in motion is defined as slave body. The prescribed displacement is applied in several increments. In each increment, the resultant force R_N at the top of superior body is calculated by summing up the reaction forces R_{Nk} on the surface related to each node k. Then,

$$R_N = \sum_k R_{Nk} \tag{3.1}$$

The existence of a reaction force R_N indicates the first contact between the bodies. The maximum initial asperities height ξ between the two middle planes, which are in contact, is determined at this step. See Figure 1 for the geometrical relations.

The normal contact force F_N at the contact interface is obtained by taking into account the real contact area A_r. The actual contact occurs at n-discrete areas A_n on the discrete boundary Γ_c^n, as shown in Figure 4. This yields

$$A_r = \sum_{n=1}^{n_c} A_n$$

when n_c asperities are in contact.

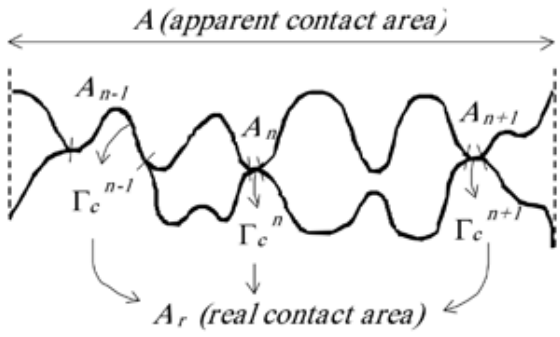

Figure 4: Contact interface (cross section)
Source: Bandeira, 2004.

The real contact pressure t_{Nn} occurs on the discrete contact surface Γ_c^n. The actual normal contact force F_N is obtained by summing up the integrals of the real normal contact pressures t_{Nn} related to the discrete area A_n at each boundary Γ_c^n. Then:

$$F_N = \sum_n \int_{\Gamma_c^n} t_{Nn} dA_n \tag{3.2}$$

In general it is difficult to determine the actual discrete contact areas and to compute F_N from (3.2). Here a different procedure is followed. Considering the equilibrium of the bodies, it is clear that the normal contact force developed at the interface is equal to the normal reactions developed at the top of superior body. Therefore, within the finite element treatment it is sufficient, instead of computing (3.2), to calculate the normal reaction force R_N. Hence:

$$F_N = R_N \tag{3.3}$$

The total contact force F_N at the interface can be distributed on the apparent contact area A to yield a uniform apparent contact pressure, p_N. Therefore, with equation (3.3),

$$PN = \frac{R_N}{A} \tag{3.4}$$

Since R_N depends on the current mean plane distance d, the penetration law is displayed as

$$P_N = P_N(d) \tag{3.3}$$

At the end of each step, the current mean plane distance d, the total reaction force R_N and the apparent contact pressure p_N are calculated. The analysis ends when the current mean plane distance d goes to zero. The numerical results after homogenization yield a microscopic contact law analogous to the theoretical law, presented in Section 2. The homogenization is computed in terms of the average normal pressure p_N. The plotted curve describes the penetration law relating the

apparent contact pressure p_N to the current mean plane distance d. See equation (3.5).

The generation of the smoothen contact surfaces with Bézier interpolations (FARIN, 1988), the procedures to obtain a statistical law and the techniques to obtain the maximum initial asperities height ξ for a generated surface were presented in detail in Bandeira, Wriggers and Pimenta (2001b).

4 Constitutive equation

The von Mises elastic-plastic constitutive law is based on the following multiplicative decomposition of the deformation gradient:

$$F = F^e F^p \tag{4.1}$$

where the superscript e and p describe the elastic and the plastic part, respectively. The elastic logarithmic strain tensor is given by

$$E^e = lnV^e, \text{ where } V^e = F^e F^{eT})^{\frac{1}{2}} \tag{4.2}$$

the elastic left stretching tensor. The elasticity is described by the following strain energy function

$$\psi(E^e) = \frac{1}{2}\kappa\vartheta^2 + \mu(\overline{E}^e : \overline{E}^e) \tag{4.3}$$

where:

$$\vartheta = \mathrm{tr}E^e \text{ and } \overline{E}^e = \mathrm{Dev}E^e \tag{4.4}$$

that leads to the following Kirchhoff-Treftz stress tensor

$$\Sigma = \mathbb{D}^e E^e, \text{ where } \mathbb{D}^e = \kappa \boldsymbol{I} \otimes \boldsymbol{I} + 2\mu(\mathbb{I} - \frac{1}{3}\boldsymbol{I} \otimes \boldsymbol{I}) \tag{4.5}$$

The logarithmic isotropic linear elastic material simplifies the volumetric-isochoric splitting. Note also that (4.5) is similar to the expression of the small strain Hooke's Law. The fourth-order tangent tensor is obtained from (4.5), as shown in detail in Pimenta (1992).

For computational purposes, the classical radial return algorithm along with the von Mises plasticity; with linear isotropic hardening is summarized below.

1) Trial step:

1. $$F_t^e = F_{i+1} U_i^{p-1};\ C_t^e = F_t^{eT} F_t^e$$

2. $$U_t^e = (C_t^e)^{1/2} = \lambda_i^e\, c_i^e \otimes c_i^e;\ \varepsilon_i = 1n\lambda_i^e;\ E_t = 1nU_t^e$$

3. $$R_t^e = F_t^e U_t^{e-1};\ b_i^e = R_t^e c_i^e$$

4. $$\vartheta_t = \mathrm{tr}(E_t);\ \overline{E}_t = \mathrm{Dev}(E_t)$$

5. $$\overline{\Sigma}_t = 2\mu\overline{E}_t;\ \overline{\sigma} = \sqrt{\frac{3}{2}\,\overline{\Sigma}_t : \overline{\Sigma}_t};\ \mathrm{F}_t = \overline{\sigma}_t - \sigma_y(\alpha_i)$$

2) Radial return algorithm

if ($F_t < 0$) then
elastic step:

1. $$\alpha_{i+1} = \alpha_i$$

2. $$U_{i+1}^p = U_i^p$$

3. $$\overline{\Sigma}_{i+1} = \overline{\Sigma}_t$$

4. $$\overline{\mathbb{D}}_{i+1} = 2\mu(\mathbb{I} - \frac{1}{3}\boldsymbol{I} \otimes \boldsymbol{I})$$

else if ($F_t \geq 0$) then
elastic-plastic step:

1. $$\Delta\alpha = \frac{\overline{\sigma}_t - \sigma_y(\alpha_i)}{3\mu + h};\ \alpha_{i+1} = \alpha_i + \Delta\alpha;\ \sigma_y(\alpha_{i+1}) = \sigma_y(\alpha_i) + h\Delta\alpha$$

2. $$\Delta E^P = \Delta\alpha \frac{3}{2\overline{\sigma}_t}\overline{\Sigma}_t;\ \Delta U^p = e^{\Delta E^P};\ F_{i+1}^p = \Delta U^p U_i^p;\ U_{i+1}^p = (F_{i+1}^{pT} F_{i+1}^p)^{\frac{1}{2}}$$

3.

$$\bar{\Sigma}_{i+1} = \frac{\sigma_{yi+1}}{\bar{\sigma}_t}\bar{\Sigma}_t$$

4.

$$\bar{\mathbb{D}}_{i+1} = 2\mu\frac{\sigma_y(\alpha_{i+1})}{\bar{\sigma}_t}(\mathbb{I} - \frac{1}{3}I\otimes I) + \frac{3\mu}{\bar{\sigma}_t^2} + (\frac{h}{3\mu + h} - \frac{\sigma_y(\alpha_{i+1})}{\bar{\sigma}_t})\bar{\Sigma}_t\otimes\bar{\Sigma}_t$$

3) add volumetric part

1.

$$\Sigma_{i+1} = k\vartheta_t I + \bar{\Sigma}_{i+1}$$

2.

$$\bar{\mathbb{D}}_{i+1} = kI\otimes I + \bar{\mathbb{D}}_{i+1}$$

The assumed linear isotropic hardening used in this paper is presented in the Figure 5.

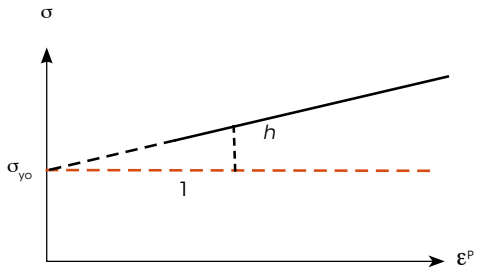

Figure 5: Constitutive equation for steel material – linear
Source: Bandeira, 2006.

Its function behavior is defined as following:

$$\sigma_y(\alpha) = \sigma_{yo} + h\varepsilon^p \qquad (4.6)$$

where σ_{yo} is the initial yield stress, $\alpha = \varepsilon^p$ is the equivalent plastic strain and h is the linear hardening parameter.

5 Numerical simulation

In this section, three numerical examples are presented to obtain an interface law for rough surfaces numerically. In these examples two blocks are considered in contact as shown in Figure 6. This is done for three-dimensional bodies in contact. The homogenization method used was presented in Section 3. The Preconditioned Bi-Conjugate Gradient Method (PBCG) is used to solve the linear equations system (PRESS, 1995). The PBCG method is used because it is more efficient, spend less computer memory to allocate the matrixes and solve linear system with non-symmetrical matrixes. The elastic-plastic material law presented in Section 4 is used in all examples. It is important to mention that each numerical laws are statistically computed curves resulted by 20 different random generated contact surfaces.

5.1 Example 1

In this first example, the number of master and slave surfaces is around 2.403 elements, and the complete mesh is around 21.627 bricks elements. Each block has the same geometry of 90mm×45mm×15mm and material properties defined by elasticity module of 70 GPa, Poisson coefficient of 0,3 and adopted initial yield stress of 200 MPa. The base of the master block is fixed and lateral displacements of both blocks are released. The hardening parameters used is defined by h = E / 100. The contact surfaces are modified according to the theory presented (BANDEIRA; WRIGGERS; PIMENTA 2001), such that the maximum initial asperities height ξ is 0,563444 mm. A uniform displacement of 4 mm is prescribed at the top of the slave block in several increments. Each analysis ends when the current mean plane distance d approaches zero. The mean plane distance goes to zero in the 93th increment of load.

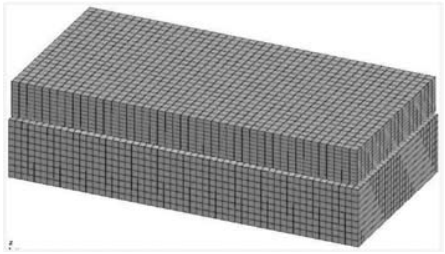

Figure 6: Contact with two deformable bodies
Source: Bandeira, 2006.

After all generated surfaces were analyzed, the mean value curve of the normal pressures is depicted (Graphic 1), which represents the constitutive interface law for different hardness.

The plastic zone developed at the master surface can be analyzed in each increment of loads by the equivalent plastic strain, presented in the algorithmic for elastoplasticity stated in Section 4 (see Figure 7).

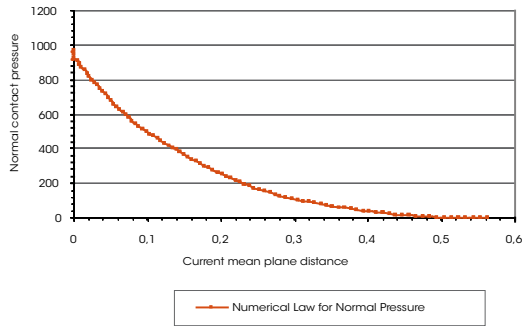

Graphic 1: Penetration behaviour
Source: Bandeira, 2006.

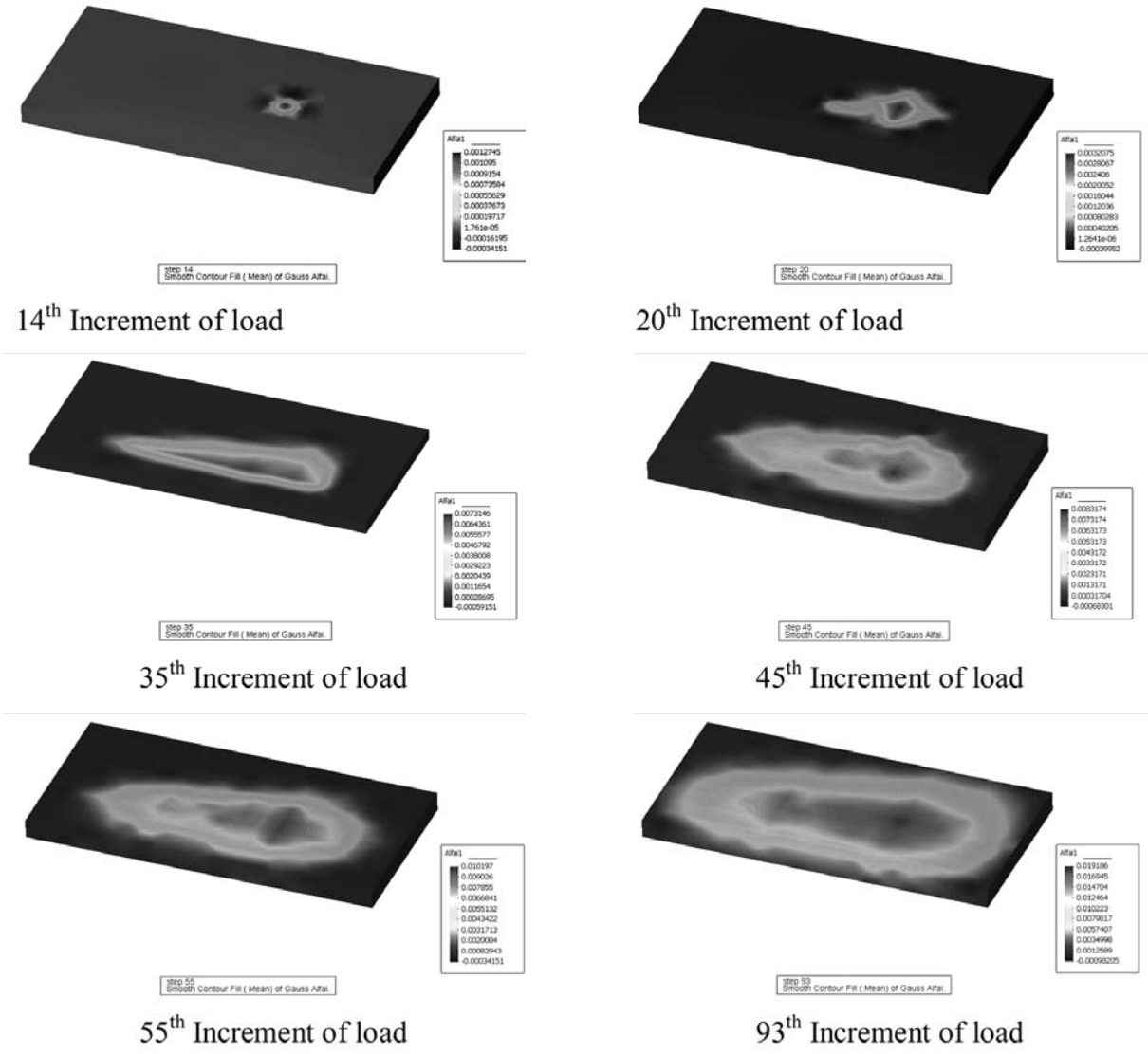

Figure 7: Plastic zone of the master surface (αi parameter)
Source: Bandeira, 2006.

5.1 Example 2

The second example is the same of the first one. The differences are that the maximum initial asperities height ξ is 0,180394 mm, and the load consists of a uniform displacement of 8 mm prescribed at the top of the slave block in several increments. Each analysis ends when the current mean plane distance *d* approaches zero. The mean plane distance goes to zero in the 35th increment of loads. After all generated surfaces were analyzed, the mean value curve of the normal pressures is depicted in Graphic 2, which represents the constitutive interface law for different hardness.

The plastic zone developed at the master surface can be analyzed in each increment of loads by the equivalent plastic strain (Figure 9).

5.1 Example 3

The last example has the same discretization of the first one. The difference is that the maximum initial asperity height ξ is 0,226265

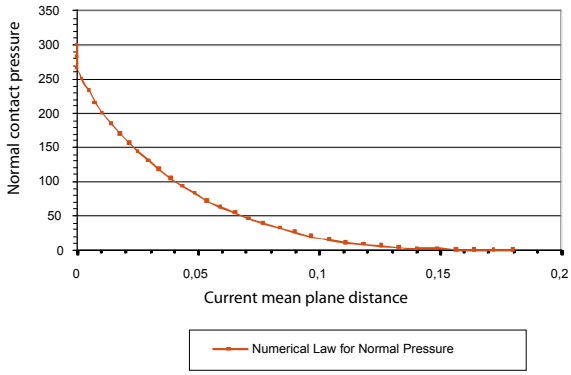

Graphic 2: Penetration behaviour
Source: Bandeira, 2006.

mm and the applied load is done in two steps. A uniform displacement of 0,24 mm is prescribed at the top of the slave block in several increments in the vertical direction. Each analysis ends when the current mean plane distance *d* approaches zero. The mean plane distance goes to zero in the 35th increment of load. After that, another increment of load, of 0,10 mm, is applied in the tangential direction, paralleled

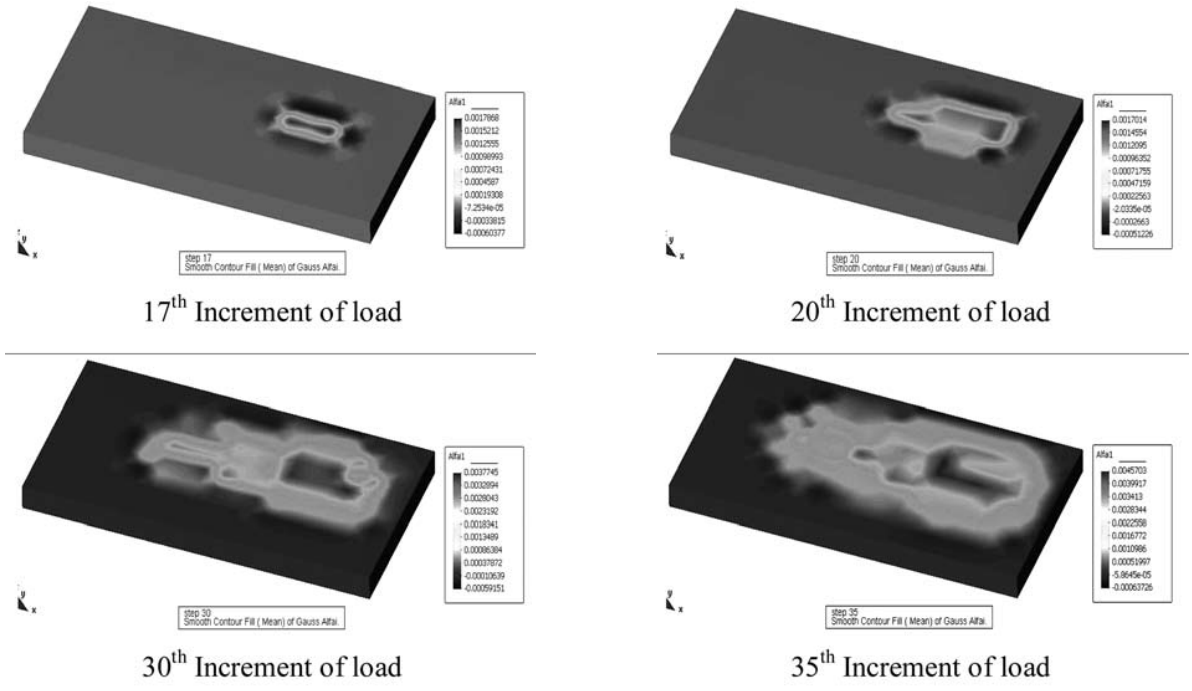

Figure 9: Plastic zone of the master surface (αi parameter)
Source: Bandeira, 2008.

to the face of 90 mm, in thirty increments. The penalty parameters used for the normal direction is around 10^5 and for the tangential direction is around 5×10^4. The friction coefficient is 0,20. After this analysis, the mean value curve of the normal pressures is depicted in Graphic 11, which represents the constitutive interface law for different hardness.

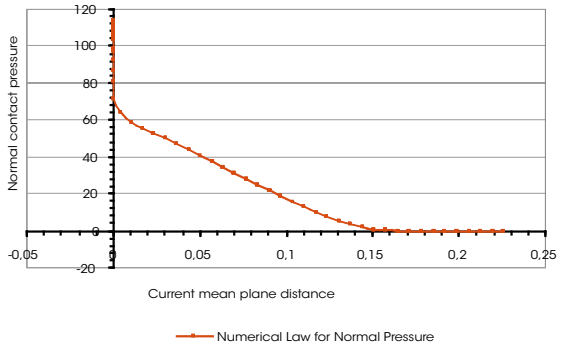

Figure 11: Penetration behaviour (*h* = E/10)
Source: Bandeira, 2008.

In this analysis the normal and tangential pressures are plotted over the displacement in each increment of load. The contact surfaces are smooth that makes the pressure very sensitive regarding the hardness. The normal and the tangential pressures behaviour are presented in Graphic 12a and 12b, respectively.

6 Final considerations

This work can be regarded as a complementary study of Bandeira et al. (2006). In that paper, the plasticity of the asperities is taken into account by assuming a constitutive equation based on associated von Mises yield function formulated in principal axes. The authors can concluded that is possible to modeling the micromechanical phenomena developed at the contact surfaces and obtained results for constitutive equations derived by numerical simulations with good agreements with the theoretical

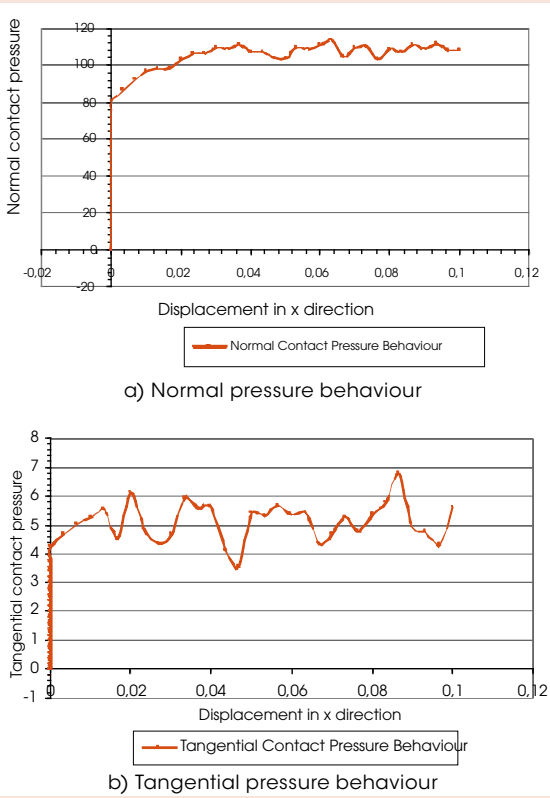

Figure 12: Constitutive Law
Source: Bandeira, 2008.

laws. In the numerical examples, the normal and tangential contact pressures are plotted to show the contact surfaces behaviour. The plasticity evolution developed at the contact surfaces are also presented in the numerical results. It can be seen that the contact surfaces developed high plasticity effects during the contact mechanics.

References

ALART, P.; CURNIER, A. A mixed formulation for frictional contact problems prone to Newton like solution methods. *Computational Methods in Applied Mechanics and Engineering*, Lausanne, Switzerland, v. 92, Issue 3, p. 353-375, 1991.

BANDEIRA, A. A.;WRIGGERS, P.; PIMENTA, P. M. *Computational analysis of contact mechanics undergoing large 3D deformation*. In: EUROPEAN CONFERENCE ON COMPUTATIONAL MECHANICS0, 2001, Krakow, Poland: ECCM, 2001a.

_____. *A constitutive law investigation of contact interfaces using a finite element method for large 3D deformation*. In: CONTACT MECHANICS INTERNATIONAL SYMPOSIUM, 3., 2001, Peniche, Portugal: CMIS, 2001b.

_____. Numerical derivation of contact mechanics interface laws using a finite element approach for large 3D deformation. *International Journal for Numerical Methods in Engineering*, 2004.

_____. *Numerical simulation of 3D contact problems under finite elastic-plastic deformation*. In: US NATIONAL CONGRESS ON COMPUTATIONAL MECHANICS, 7., 2003, Albuquerque, New Mexico, USA, 2003.

_____. A 3D study of the contact interface behavior using elastic-plastic constitutive equations. In: WRIGGERS, P.; NACKENHORST, U. (Org.). *Analysis and Simulation of Contact Problems*. Ed. 1, Berlin: Springer, 2006. v. 27. p. 313-324.

BERTSEKAS, D. P. *Constrained optimization and Lagrange multiplier methods*. 1. ed. New York: Academic Press, 1984.

_____. *Nonlinear programming*. 1 ed. Belmont: Athena Scientific, 1995.

CURNIER, A. A Theory of Friction. *International Journal for Solids Structures*, v. 20, Ed. 1, p. 637-647, 1984.

EVSEEV, D. G.; MEDVEDEV, B. M.; GRIGORIYAN, G. G. Modification of the elastic-plastic model for the contact of rough surfaces. *Wear*, v. 150, Ed. 1, p. 79-88, 1991.

FARIN, G. *Curves and surfaces for computer aided geometric design*: a practical guide. Ed. 1, Arizona: Department of Computer Science, Arizona State University, 1988.

FLETCHER, R. *Practical methods of optimization*. 2. ed. Chichester: John Wiley & Sons, 2000. 2v.

GREENWOOD, J. A; WILLIAMSON, J. B. P. Contact of nominally flat surfaces. Proceedings of the Royal Society of London. Series A, Mathematical and Physical Sciences, U.S.A., v. 295, n. 1442, p. 300-319, dec. 1966.

HEEGAARD, J. H.; CURNIER, A. An augmented Lagrangian method for discrete large-slip contact problems. *International Journal for Numerical Methods in Engineering*, v. 36, Ed. 1, p. 569-93, 1993.

KARDESTUNCER, H; NORRIE, D. H. *Finite element handbook*. 1. ed. U.S.A: McGRAW-HILL Book Company, 1987.

KRAGELSKY, I. V.; DOBYCHIN, M. N.; KOMBALOV, V. S. *Friction and wear*: calculation methods. Translated from The Russian by N. Standen. 1. ed. New York: Pergamon Press, 1982.

LAURSEN, T. A.; MAKER, B. N. An augmented Lagrangian quasi-Newton solver for constrained nonlinear finite element applications. *International Journal for Numerical Methods in Engineering*, v. 38, Ed. 1, p. 3571-90, 1995.

LAURSEN, T. A.; SIMO, J. C. A Continuum-Based Finite Element Formulation for the Implicit Solution of Multibody, Large Deformation Frictional Contact Problems. *International Journal for Numerical Methods in Engineering*, v. 36, Issue 20, p. 3451-85, 1993a.

_____. Algorithmic symmetrization of coulomb frictional problems using augmented Lagrangians. *Computer Methods in Applied Mechanics and Engineering*, v. 108, Issue 108, p. 133-46, 1993b.

LUENBERGER, D. G. *Linear and nonlinear programming*. 2. ed. Massachusetts: Addison-Wesley Publishing Company, 1984.

ODEN, J. T.; PIRES, E. B. Algorithms and numerical results for finite element approximations of contact problems with non-classical friction laws. *Computer & Structures*, v. 19, p. 137-147, 1983.

PIMENTA, P. M. Finite deformation soil plasticity on principal axes. In: INTERNATIONAL CONFERENCE ON COMPUTATIONAL PLASTICITY, FUNDAMENTALS AND APPLICATIONS, 3., 1992, Swansea, U. K. *Proceedings*..., Swansea, U.K.: Pineridge Press Limited, 1992. p. 859-870.

PRESS, W. H. *Numerical recipes in C*: the art of scientific computing. 2. ed. Cambridge: University Press, 1995.

SIMO, J. C.; LAURSEN, T. A. An augmented Lagrangian treatment of contact problems involving friction. *Computers & Structures*, vo. 42, p. 97-116, 1992.

TABOR, D. Friction: the present state of our understanding. *Journal of Lubrication Technology*, vo. 103, p. 169-116, 1981.

WRIGGERS, P. Finite element algorithms for contact problems. *Archives of Computational Methods in Engineering*, v.2, n. 4, p. 1-49, 1995.

_____.; SIMO, J. C. A note on tangent stiffness for fully nonlinear contact problems. *Communications in Applied Numerical Methods*, v.1, p. 199-203, 1985.

_____.; _____. TAYLOR, R. L. Penalty and augmented Lagrangian formulations for contact problems. In: NUMETA CONFERENCE, 85., 1985, Rotterdam. *Proceedings*... Rotterdam: Balkema, 1985.

_____.; VU VAN, T.; STEIN, E. Finite element formulation of large deformation impact-contact problems with friction. *Computers & Structures*, v. 37, p. 319-31, 1990.

_____.; ZAVARISE, G. On the application of augmented lagrangian techniques for nonlinear constitutive laws in contact interfaces. *Comm. Num. Meth. Engng.*, v. 9, p. 815-24, 1993.

YOVANOVICH, M. M. Thermal Contact Correlations. *AIAA Paper*, Palo Alto, v. 16, Ed. 1, p. 81-1.164, 1981.

ZAVARISE, G; SCHREFLER, B. A; WRIGGERS, P. Consistent formulation for thermomechanical contact based on microscopic interface law. In: COMPLAS, 3., 1992. *Proceedings*... D. R. J. Owen, E. Hilton, E. E. Oñate, Pineridge Press, 1992.

Recebido em 7 fev. 2008 / aprovado em 23 abr. 2008

Para referenciar este texto

BANDEIRA, A. A.; PIMENTA, P. M.; WRIGGERS, P. A 3D contact investigation of rough surfaces considering elastoplasticity. *Exacta*, São Paulo, v. 6, n. 1, p. 109-118, jan./jun. 2008.